Published in final edited form as:
*Acta Biomater*. 2011 June ; 7(6): 2410–2417. doi:10.1016/j.actbio.2011.02.029.

# Glyoxal Crosslinking of Cell-Seeded Chitosan/Collagen Hydrogels for Bone Regeneration

**Limin Wang** and **Jan P. Stegemann***
Department of Biomedical Engineering, University of Michigan, Ann Arbor, MI 48109, USA

## Abstract

Chitosan and collagen are natural biomaterials that have been used extensively in tissue engineering, both separately and as composite materials. Most methods to fabricate chitosan/collagen composites use freeze drying and chemical crosslinking to create stable porous scaffolds, which subsequently can be seeded with cells. In this study, we directly embedded human bone marrow stem cells (hBMSC) in chitosan/collagen materials by initiating gelation using β-glycerophosphate at physiological temperature and pH. We further examined the use of glyoxal, a dialdehyde with relatively low toxicity, to crosslink these materials and characterized the resulting changes in matrix and cell properties. The cytocompatibility of glyoxal and the crosslinked gels were investigated in terms of hBMSC metabolic activity, viability, proliferation, and osteogenic differentiation. These studies revealed that glyoxal was cytocompatible at concentrations below about 1 mM for periods of exposure up to 15 h, though the degree of cell spreading and proliferation were dependent on matrix composition. Glyoxal-crosslinked matrices were stiffer and compacted less than uncrosslinked controls. It was further demonstrated that hBMSC can attach and proliferate in 3D matrices composed of 50/50 chitosan/collagen, and that these materials supported osteogenic differentiation in response to stimulation. Such glyoxal-crosslinked chitosan/collagen composite materials may find utility as cell delivery vehicles for enhancing the repair of bone defects.

### Keywords

glyoxal; crosslinking; collagen; chitosan; mesenchymal stem cell; bone regeneration

## 1. Introduction

Chitosan and collagen type I composite materials have been proposed for many regenerative applications in tissues as diverse as bone [1], ligament [2], skin [3], and blood vessels [4]. Both of these materials are derived from natural sources and have key features that make them attractive in regenerative medicine, including compatibility with implantation and the ability to be degraded over time. Type I collagen is a main structural protein in many tissues and contains a variety of bioactive sites that promote cell attachment [5,6] and regulate cell differentiation [7,8]. Chitosan is a polysaccharide derived from the exoskeleton of crustaceans, which has been commercialized in wound-healing applications because of its tissue adhesive and antibacterial properties [9]. Composites of these materials have been

*Corresponding Author: Jan P. Stegemann, Department of Biomedical Engineering, University of Michigan, 1101 Beal Ave, Ann Arbor, MI 48109, Tel: 734-764-8313, Fax: 734-647-4834, jpsteg@umich.edu.

explored because they offer the opportunity to integrate the benefits of each component while avoiding the drawbacks. For example, such composites offer good cell attachment because of the collagen component, while also being stable and resistant to rapid remodeling because of the chitosan component. In bone tissue engineering, chitosan/collagen composites have been shown to enhance the mechanical stiffness of scaffolds and to induce osteogenic differentiation of bone marrow stem cells, relative to either pure component [10].

A common method to create chitosan/collagen composite scaffolds involves a freeze-drying process that results in a sponge-like network with interconnected pores [10,11]. Chitosan/collagen sponges often require an additional crosslinking step to stabilize hydrogels and enhance their mechanical properties and prevent degradation. Glutaraldehyde is one of the most widely used reagents to crosslink both chitosan and collagen due to its high effectiveness in creating irreversible crosslinking bonds [12,13]. In most cases, cells cannot be incorporated into such materials during fabrication because of the high cytotoxicity of glutaraldehyde, and therefore must be seeded onto the exterior of scaffolds post-fabrication. More recently, injectable formulations of chitosan/collagen materials have been developed using β-glycerophosphate (β-GP) to initiate gelation [14,15]. In this case the β-GP helps to create physical crosslinks in the polymers, but eventually leaks out of the gel. Although the mechanism is not entirely clear, it is thought that β-GP plays two important roles in chitosan/collagen composite gel formation. First, it acts as a proton receiver from the positively charged chitosan at elevated temperature and thereby induces chitosan gelation [16]. Second, β-GP is a weak base and therefore can neutralize weakly acidic collagen type I solutions and initiate self-assembly of a fibrous network that mimics native collagen conformation. In a previous study, we showed that β-GP-initiated chitosan/collagen composites could be created at physiological pH and temperature, and that hBMSC remained viable and continued to proliferate when embedded in such materials at the time of fabrication [14].

Composite chitosan/collagen gels created using β-GP-initiated gelation are however mechanically weak, because they are stabilized only by electrostatic bonds, as opposed to covalent or ionic bonds [16]. It has been reported that the small aldehyde glyoxal can be used in combination with β-GP to create stable and biocompatible chitosan hydrogels for cartilage regeneration [17]. This study showed that a human epithelial cell line (HEK293) could be embedded in 3D gels and tolerated up to 0.15 mM glyoxal while retaining their viability and ability to proliferate in culture. Calf chondrocytes were also subsequently encapsulated in such gels for in vivo evaluation. Although glyoxal is an aldehyde and has been implicated in contact dermatitis [18], it exhibits generally lower cytotoxicity when compared to glutaraldehyde [19]. In the current study, we have investigated the use of glyoxal to crosslink and therefore stabilize chitosan/collagen composite materials gelled with β-GP and seeded with hBMSC. Our study includes examination of the effects of glyoxal on both the cellular and matrix components of these materials. In addition, we have assessed the osteogenic potential of hBMSC when cultured in 3D glyoxal-crosslinked chitosan/collagen hydrogels and stimulated by osteogenic supplements. We expect that such crosslinked chitosan/collagen materials will find utility in bone tissue engineering because they provide a stable osteoconductive matrix that also promotes cell attachment.

## 2. Materials and Methods

### 2.1 Preparation of chitosan/collagen hydrogels

Chitosan/collagen composite gel formation was induced by β-GP using our previously published protocol [14]. In brief, 4.0 mg/ml bovine Type I collagen (MP Biomedicals, Solon, OH) dissolved in 0.02 N acetic acid (Sigma, St. Louis, MO) was mixed with 2.0 wt% chitosan (93% DDA; BioSyntech, Quebec, Canada) dissolved in 0.1 N acetic acid to prepare

four chitosan/collagen mass ratios: 0/100, 25/75, 50/50, and 75/25. A chitosan/collagen ratio of 100/0 was not used because our previous work has shown that this pure chitosan formulation does not support cell attachment [14]. The matrix solution was then diluted with a pre-cooled 58 wt% β-GP stock solution containing hBMSC and/or glyoxal, to achieve the desired cell density, glyoxal concentration and final concentration of a 5 wt% β-GP. Gelation was then initiated by incubation of this matrix mixture at 37 °C for 30 min.

### 2.2 Evaluation of glyoxal cytotoxicity in 2D cultures

hBMSC (Lonza Inc., Walkersville, MD) were thawed and cultured in complete medium consisting of Dulbecco's Modified Eagle Medium - low glucose (DMEM-LG; Invitrogen, Carlsbad, CA), 10% MSC-qualified fetal bovine serum (FBS; Invitrogen, Carlsbad, CA), and 1% penicillin/streptomycin (PS; Invitrogen). To evaluate the cytotoxicity of glyoxal solutions, hBMSC at passage 5 were seeded at a density of 12,500 cells per well in 96-well plates and cultured for 24 h in complete medium. The medium was then replaced with 100 μl of serum-free DMEM containing a range of concentrations of glyoxal: 0, 0.001, 0.01, 0.1, 1.0, 10.0 and 100 mM. Cytotoxicity assays were conducted using a MTT [3-(4,5-Dimethylthiazol-2-yl)-2,5-diphenyltetrazolium bromide] cell proliferation kit (Roche Applied Science, Indianapolis, IN) according to the manufacturer's instructions after 1, 5 and 15 h incubations with glyoxal. In brief, 10.0 μl of MTT labeling reagent was added to each well followed by a 4 h incubation at 37 °C. 100 μl of the solubilization solution was then added into each well for 15 h to dissociate the purple formazan crystals. The plates were read at 550 and 690 nm using a spectrophotometer. The difference in absorbance values between 550 and 690 nm indicated the metabolic activity of the cells, which is proportional to cell number. Four samples of each treatment type were analyzed.

### 2.3 Cell viability on 2D gel films and in 3D gel matrices

To create crosslinked gel films, chitosan/collagen solutions containing chitosan/collagen mass ratios of 0/100, 25/75, 50/50, and 75/25 and 1.0 mM glyoxal were cast onto 48-well plates using 100 μl of solution per well. After 30 min of gelation, gels were rinsed three times for 10 min with phosphate buffered saline (PBS) containing 10 mM glycine to quench glyoxal residues. hBMSC were then seeded on the top surface of the gels at 5,000 cells/cm$^2$ and were cultured in complete medium for three days before being assayed for cell viability and DNA content to determine cell numbers. To create cell-seeded 3D hydrogel matrices, hBMSC were added to solutions containing the appropriate matrix component ratios at a concentration of $1.0\times10^6$ cells/ml. Gelled constructs were cultured for 1 or 9 days in complete medium before being assayed for cell viability. A commercially available vital staining kit (Live/Dead®, Molecular Probes, Eugene, OR) was used to assess the viability of cell populations both on 2D gel substrates and within 3D gels. Samples were washed in sterile PBS and incubated at room temperature for 1 h in a solution containing 4.0 μM calcein-AM and 4.0 μM ethidium homodimer-1 in PBS. After incubation, constructs were washed and then imaged using fluorescent microcopy. Laser scanning confocal microscopy was used to image the matrix of the constructs. For 3D gels, image scans were captured at a horizontal plane 200 μm below the gel surface, in order to ensure that fully embedded cells were being imaged. For quantitation of cell numbers in both 2D and 3D samples, DNA was extracted in 4.0 M guanidine hydrochloride solution [14] and measured using a commercially available DNA assay (PicoGreen kit, Invitrogen) following the manufacturer's protocol.

### 2.4 Scanning electron microscopy

Each of the four chitosan/collagen formulations were examined using scanning electron microscopy (SEM), using both uncrosslinked and 1.0 mM glyoxal-crosslinked samples of each formulation. Unseeded gel samples were snap-frozen in liquid nitrogen and then

freeze-dried overnight. Dried gels were cut with a sharp blade to expose the internal microstructure of the constructs and were then sputter coated with platinum-gold. Samples were imaged at 15 kV using a Nova Nanolab scanning electron microscope (FEI Inc., Hillsboro, OR).

### 2.5 Rheological measurements

The formulation containing 50/50 chitosan/collagen matrices was evaluated by gel rheometry using an AR-G2 rheometer (TA Instruments, New Castle, DE). Both uncrosslinked and 1.0 mM glyoxal-crosslinked matrices were evaluated. The gel precursor components were combined and 300 μL of this solution was loaded onto a Peltier stage preheated to 37 °C. A 20-mm steel parallel plate was used with a gap height of 800 μm. A small amount of mineral oil was applied around the sample to minimize water evaporation during the testing process. A time sweep was performed over the course of 30 min with constant angular frequency and strain percentage values of 1 rad/s and 1.0%, respectively. Full polymerization was defined as the phase of the curve when the values of G′ plateaued. Four to six samples of each group were tested, and the storage (G′) and loss (G″) moduli at 30 min were reported.

### 2.6 Gel compaction assay

The change in gel size over time was monitored in 50/50 chitosan/collagen constructs seeded with hBMSC at a concentration of $1.0 \times 10^6$ cells/ml. Gels were fabricated as described above. Both uncrosslinked and 1.0 mM glyoxal-crosslinked matrices were evaluated. Formed gels were cultured in complete medium for 19 days and images were taken every 2 days to measure changes in gel size, as reflected by the change in the imaged area of the construct. ImagePro software (Media Cybernetics, Bethesda, MD) was used to calculate gel area, and the degree of gel compaction was defined as the change in area over time. Four samples of each formulation were examined.

### 2.7 Induction of osteogenic differentiation of hBMSC

An osteogenic medium consisting of complete DMEM supplemented with 100 nM dexamethasone (Sigma), 5.0 mM β-GP, and 50 μg/ml ascorbic acid 2-phosphate (Sigma) was used to stimulate osteogenic differentiation of hBMSC embedded in 3D chitosan/collagen gels. Cells were embedded as described above at a concentration of $1.0 \times 10^6$ cells/ml. Both uncrosslinked and 1.0 mM glyoxal-crosslinked matrices were evaluated. Gels were cultured for 19 days in osteogenic medium and were compared to control samples cultured in complete DMEM without osteogenic supplements. Media were changed every two days. ALP activity, calcium content, and gene expression were examined at days 1, 9, and 19 as described in the following sections.

### 2.8 Quantitation of alkaline phosphatase activity and calcium content

Samples were snap frozen in liquid nitrogen, pulverized, and then lysed in 500 μl of 0.2% Triton X-100 (Sigma) using two freeze–thaw cycles. Alkaline phosphatase (ALP) activity was measured using a previously described protocol [20]. In brief, 20 μl of the sample lysate was incubated for 15 min with 80 μl of 1.5 M 2-amino-2-methyl-1-propanol (AMP; Sigma) buffer at pH 10.3 containing 5.0 mM p-nitrophenol phosphate substrate (Sigma). Samples were read spectrophotometrically at 405 nm. Serial dilutions of 0–20 nM p-nitrophenol (Sigma) in Triton solution served as a standard curve. Calcium quantification was performed using an orthocresolphthalein complex one (OCPC) method as previously described [20]. In brief, pulverized samples were digested in 1.0 ml of 1.0 N acetic acid for 12 h. Twenty microliters of the digested solution was then incubated for 10 min at 23 °C with 250 μl of a working solution consisting of 0.05 mg/ml OCPC solution and ethanolamine/boric acid/8-

hydroxyquinoline buffer (Sigma). Samples were read spectrophotometrically at 575 nm. Both ALP activity and calcium content were normalized to DNA content. Four samples of each treatment type were analyzed.

### 2.9 RNA isolation and RT-PCR analysis

Samples were snap frozen in liquid nitrogen and pulverized for RNA extraction using previously published methods [21]. In brief, sample powders were mixed with 600 μl pre-warmed cetlytrimethylammonium bromide (CTAB) extraction buffer. An equal volume of chloroform-isoamyl alcohol (24:1) (Fisher Scientific, Pittsburgh, PA) was added and mixed, followed by centrifugation for 5 min at 15,000 ×g at room temperature. An equal amount of isopropanol (IPA) was then added to precipitate RNA. Total RNA was dissolved in 30 μl RNase-free water after an ethanol wash for further purification using a Qiagen RNeasy Mini kit (Qiagen Inc., Valencia, CA). For quantitative RT-PCR, a High-Capacity cDNA Archive kit (Applied Biosystems *Inc.*, Foster City, CA) was first used to convert messenger RNA (mRNA) to complementary DNA (cDNA). TaqMan gene expression assay kits (Applied Biosystems) were used to determine transcript levels of glyceraldehyde 3-phosphate dehydrogenase (GAPDH, Hs99999905_m1), type I collagen (CI, Hs00164004_m1), bone sialoprotein (BSP, Hs00173720_m1), and osterix (OSX, Hs00541729_m1) using an Applied Biosystems 7500 Fast System. The $2^{-\Delta\Delta Ct}$ method was used to evaluate relative mRNA expression levels for each target gene [22]. Samples were normalized first by the difference (ΔCt) between the Ct values of target genes and the GAPDH gene and then by subtracting the ΔCt value of the calibrator sample, their respective Ct values at day 1, to obtain ΔΔCt values. Four samples of each treatment type were analyzed.

### 2.10 Statistical analysis

All quantitative data were processed using analysis of variance (ANOVA) followed by Tukey's Significant Difference post-hoc tests. The level of statistical significance was set at 5% ($p<0.05$).

## Results

### 3.1 Cytotoxicity of glyoxal in 2D and 3D

To investigate the effect of glyoxal on cell viability, hBMSC were seeded on 2D tissue culture-treated plastic surfaces and were directly exposed to different concentrations of glyoxal for up to 15 h, as shown in Figure 1A. The values of metabolic activity for control samples (no glyoxal) are indicated in the legend of this figure. In general, the metabolic activity of hBMSC was not affected by glyoxal at low concentrations, but there was a relatively clear cut-off point above which cellular activity decreased. The effect of glyoxal also was dependent on exposure time. At a 1 h incubation time, cell metabolic activity was unaffected up to concentrations of 10 mM ($p > 0.05$), though at increasing exposure time this value was reduced to around 1 mM. hBMSC also were cultured on the surface of chitosan/collagen gels that had been crosslinked with 1.0 mM glyoxal. Figures 1B to 1E show viability staining of hBMSC at day 3 on the surface of such gels with increasing chitosan contents. Cell viability was over 95% in all groups, suggesting that residual glyoxal did not affect cell function. It was also observed that cells spread and proliferated to a greater degree with increasing collagen content (Figures 1B to 1E). Differences in cell proliferation were quantified using DNA content (Figure 1F), and cell number was higher in pure collagen than all other groups ($p < 0.05$). In addition, cell number in the 25/75 group was significantly greater than in the 75/25 group ($p < 0.05$).

Viability of hBMSC in a range of formulations of 3D chitosan/collagen matrices was also evaluated, as shown in Figure 2. Cells were added to the matrix solution during gelation

such that they were embedded directly in the matrix, and both uncrosslinked and 1.0 mM glyoxal crosslinked samples were examined. In 3D gels, hBMSC demonstrated high cell viability (>90%) after gelation at day 1 in both crosslinked and uncrosslinked gels. Some dead cells (indicated by red nuclei in Fig. 2) were sporadically observed in crosslinked gels, however in general most cells survived the embedding and crosslinking process. In addition, there was no significant difference in cell viability between the different chitosan/collagen ratios at day 1. Similarly, after 9 days in culture cells in all groups maintained high viability (>90%), with no differences observed between the crosslinking treatments or the different chitosan/collagen ratios. By day 9, hBMSC in most gels had clearly spread within the 3D matrix and had adopted an elongated morphology. The single exception was that cells in crosslinked 75/25 chitosan/collagen gels retained a rounded morphology, though their viability was still high.

### 3.2 SEM analysis

Examination of the microstructure of chitosan/collagen matrices using SEM revealed that all gels exhibited an interconnected porous structure after gelation, as shown in Figure 3. As expected, pure collagen gels (panels A, B) consisted of a fibrous network, with little difference between the uncrosslinked and glyoxal crosslinked matrices. Gels containing chitosan (panels C-H) had a progressively less fibrillar structure as chitosan content increased. At chitosan/collagen ratios of 25/75 (panels C, D) and 50/50 (panels E, F), the chitosan matrix was observed dispersed throughout collagen fibers. At the highest chitosan/collagen ratio (75/25; panels G,H), the gels exhibited a sponge-like structure with much larger pores than the gels containing lower chitosan content, in both uncrosslinked and crosslinked groups. Panels I and J of Figure 3 are lower magnification images of these gels, and show that crosslinking of 75/25 gels changed the matrix morphology. Crosslinked gels had even larger pores and a plate-like structure, with very little evidence of fibrillar matrix, whereas uncrosslinked gels had a more uniform appearance with occasional fibrous struts.

### 3.3 Gel compaction and stiffness

Figure 4A shows the change in gel dimension over time of 50/50 chitosan/collagen matrices seeded with $1.0 \times 10^6$ hBMSC/ml and cultured for 19 days. In general, uncrosslinked gels compacted more rapidly and to a greater extent than glyoxal crosslinked gels, and the surface area was significantly different ($p<0.05$) at all time points except day 1. Uncrosslinked gels began to compact early in the culture period and continued to compact at a constant rate for about two weeks. In contrast, the crosslinked gels compacted only moderately until about day 10, at which time the rate of compaction increased. Compaction of both gel types plateaued at approximately day 15, and at the end of the culture period the uncrosslinked gels had compacted to about half the size of their crosslinked counterparts. Figure 4B shows the storage ($G'$) and loss ($G''$) moduli of 50/50 chitosan/collagen gels measured directly after gelation. Relative to uncrosslinked controls, glyoxal crosslinking caused a 6-fold increase in the stiffness of the gels as represented by the storage modulus ($p<10^{-4}$), but had little effect on the loss modulus.

### 3.4 DNA content, alkaline phosphatase activity, calcium deposition, and gene expression

Figure 5 shows cell activity data for hBMSC embedded in 50/50 chitosan/collagen matrices at a concentration of $1.0 \times 10^6$ cells/ml and exposed to osteogenic or control culture conditions for a period of 19 days. The DNA content (panel A) is reflective of cell number and therefore an increase suggests proliferation of the embedded cells. The increase was more pronounced in uncrosslinked gels, and osteogenic medium also resulted in higher DNA contents. In control medium, the DNA content of uncrosslinked gels was significantly higher at both day 9 ($p<10^{-4}$) and day 19 ($p<10^{-10}$), relative to day 1, showing about a 2-fold increase by day 19. In osteogenic medium, the DNA content of uncrosslinked gels also

increased significantly relative to both the day 1 control ($p<10^{-10}$) and to the crosslinked gels ($p<10^{-4}$), yielding about a 3-fold increase over 19 days ($p<10^{-10}$). In contrast, crosslinked gels showed no statistically significant difference in DNA content between control and osteogenic groups at either time point, though the DNA content in these gels was approximately 1.5-fold higher at day 19 than at day 1 ($p<10^{-3}$).

Alkaline phosphatase (ALP) activity, shown in Figure 5B, did not change significantly when hBMSC-seeded gels were cultured in control medium. However, when exposed to osteogenic medium hBMSC in both uncrosslinked and crosslinked gels showed markedly increased activity. ALP activity in uncrosslinked samples was about 8-fold higher than control at day 9 and maintained this level throughout the culture period ($p<10^{-10}$). In crosslinked samples, ALP activity was about 5-fold higher than control at day 9 ($p<10^{-4}$), and continued to increase to 10-fold higher than control at day 19 ($p<10^{-10}$). ALP in uncrosslinked samples was statistically greater that in crosslinked samples at day 9 ($p<10^{-8}$), but at day 19 there was no significant difference between these groups.

Calcium deposition data are shown in Figure 5C. The calcium content of all constructs tended to increase with time in both crosslinked and uncrosslinked groups, and the osteogenic medium resulted in a marked increase in calcium deposition by day 19. In osteogenic medium, there was no significant difference in calcium content between uncrosslinked and glyoxal crosslinked gels at either time point, and by day 19 the calcium levels were about 7-fold higher than at day 1. In control medium, calcium content showed a significant increase from day 1 to day 19 in both crosslinked ($p<10^{-8}$) and uncrosslinked groups ($p<0.05$), and by day 19 crosslinked samples had a 2-fold higher calcium content than their uncrosslinked counterparts ($p<10^{-4}$).

Expression of key osteogenic genes also was monitored in 3D chitosan/collagen gels, as shown in Figure 5D-5F. There was no significant difference in osteogenic gene expression detected in the control groups at any time point, however osteogenic medium greatly enhanced osteogenesis in both uncrosslinked and crosslinked gels. Specifically, in osteogenic medium, levels of osterix in uncrosslinked gels (Fig. 5D) increased about 50-fold from day 1 to day 9 ($p<10^{-10}$), before declining to about a 10-fold increase by day 19 ($p<10^{-4}$). In crosslinked gels, osterix expression was approximately 20-fold higher at both time points, compared to day 1 ($p < 10^{-7}$). In uncrosslinked matrices, bone sialoprotein gene expression (Fig. 5E) increased to about 95-fold higher at day 9 than at day 1 ($p<10^{-4}$), and further increased to about a 150-fold higher expression at day 19 ($p<10^{-8}$). Crosslinked gels exhibited little change by day 9, but at day 19 showed about a 50-fold increase in bone sialoprotein expression, relative to day 1 ($p<0.05$). Type I collagen gene expression (Fig. 5F) clearly decreased in 3D chitosan/collagen matrices in both control medium and in osteogenic medium ($p<10^{-3}$). The decrease was evident at day 9 in culture, and levels did not change significantly by day 19.

## Discussion

The goal of the present study was to evaluate the effect of glyoxal crosslinking on chitosan/collagen matrices in the presence of embedded hBMSC. In contrast to other larger aldehydes, cells were not damaged by exposure to glyoxal when concentrations were kept below approximately 1 mM, even at exposure times of up to 15 h. Cytocompatibilty was demonstrated by the steady metabolic activity, normal degree of cell spreading, and high viability of hBMSC when exposed to glyoxal or cultured on glyoxal-crosslinked 2D chitosan/collagen substrates. In addition, it was shown that hBMSC could be incorporated directly into 3D chitosan/collagen matrices and that the cells survived the crosslinking process. Full gelation of the constructs required only about 30 min before the gels were

washed to remove excess glyoxal. It is also likely that chitosan and collagen have a protective effect on cells, since each of these polymers contains abundant amine groups that act as a substrate for glyoxal and may therefore shield the cells from cytotoxic effects. It has been observed previously that glyoxal-induced apoptosis in osteoblastic cells is reduced in the presence of type I collagen [23]. It is therefore likely that higher glyoxal concentrations can be used to crosslink 3D matrices in the presence of cells, though we limited our study to lower concentrations to ensure cytocompatibility.

The ratio of chitosan to collagen in 3D matrices was shown to affect cell function, including cell attachment, spreading, proliferation, and osteogenic differentiation. A high chitosan content, as in the 75/25 formulation, reduced cell spreading and proliferation in both 2D and 3D geometries. This observation is consistent with our previous study using uncrosslinked matrices [14], in which pure chitosan matrices did not support cell proliferation and resulted in cell death over time. In the present work, SEM images suggested that fewer collagen fibrils were exposed as the chitosan/collagen ratio increased. Therefore it is possible that reduced access to the binding sites on collagen resulted in the observed decrease in cell spreading. Chitosan is a polysaccharide and lacks cell attachment sites, however it has been shown that this material supports osteogenic differentiation of hMSC [10,14]. We chose a matrix formulation of 50/50 chitosan/collagen for the evaluation of osteogenic differentiation, in order to capitalize on both the cell adhesion characteristics of collagen and the osteogenic properties of chitosan. Culture of such 3D hBMSC-seeded matrices in osteogenic medium showed that they clearly supported osteogenic differentiation, as evidenced by increased ALP activity and calcium deposition, as well as higher osterix and BSP gene expression in the osteogenic medium compared to control medium.

Crosslinking of the 3D matrices with glyoxal also was shown to modulate cell function. Cell proliferation in crosslinked gels was lower than in uncrosslinked controls, as indicated by lower DNA content. Again, this difference may be attributable to decreased availability of cell binding sites in crosslinked materials, since the chitosan and collagen may be bonded together by the action of glyoxal. In addition, crosslinked gels are stiffer and may resist cell-mediated remodeling processes to a greater degree than uncrosslinked gels, however the interactions between matrix stiffness and remodeling are complex, and the effect on the proliferation of hBMSC is not fully understood. Composite matrices compacted over time through a collagen and cell-mediated process, as evidenced by the fact that pure chitosan matrices and acellular matrices do not compact [14]. The degree of compaction was correlated with the DNA content of matrices, indicating a relationship between the number of cells in the matrix and its degree of remodeling. Collagen density also has been implicated in the degree of compaction [24], and it may also have been affected by the stiffness of the matrix [25]. Crosslinked gels in some cases presented a delayed response to osteogenic stimulation, but exhibited similar osteogenic responses compared to uncrosslinked controls by the end of the culture period, indicating that glyoxal crosslinking did not reduce the osteoconductive properties of chitosan/collagen materials.

## Conclusions

Taken together, our results show that glyoxal-crosslinked chitosan/collagen materials can support the viability, proliferation and activity of hBMSC. In addition, these matrices are stiffer than their uncrosslinked counterparts and undergo less remodeling by embedded cells. A 50/50 chitosan/collagen material crosslinked with 1.0 mM glyoxal for 30 min was shown to produce a material that supports osteogenic differentiation of hBMSC in response to standard stimuli. Such materials may have utility for matrix-enhanced delivery of progenitor cells to sites of bone damage, to accelerate bone healing and achieve more complete repair.

## Acknowledgments

The authors thank Suraj Kachgal and Dr. Andy Putnam (Dept. Biomedical Engineering, University of Michigan) for their assistance with gel rheometry measurements. This project was supported by the National Institute of Arthritis and Musculoskeletal and Skin Diseases through grant R01-AR053231.

## References

1. Arpornmaeklong P, Suwatwirote N, Pripatnanont P, Oungbho K. Growth and differentiation of mouse osteoblasts on chitosan-collagen sponges. Int J Oral Maxillofac Surg. 2007; 36:328–37. [PubMed: 17223012]
2. Peng L, Cheng X, Wang J, Xu D, Wang G. Preparation and evaluation of porous chitosan/collagen scaffolds for periodontal tissue engineering. J Bioact Compat Polym. 2006; 21:207.
3. Ma L, Gao C, Mao Z, Zhou J, Shen J, Hu X, et al. Collagen/chitosan porous scaffolds with improved biostability for skin tissue engineering. Biomaterials. 2003; 24:4833–41. [PubMed: 14530080]
4. Zhu C, Fan D, Duan Z, Xue W, Shang L, Chen F, et al. Initial investigation of novel humanlike collagen/chitosan scaffold for vascular tissue engineering. J Biomed Mater Res A. 2009; 89:829–40. [PubMed: 19165794]
5. Jokinen J, Dadu E, Nykvist P, Kapyla J, White DJ, Ivaska J, et al. Integrin-mediated cell adhesion to type I collagen fibrils. J Biol Chem. 2004; 279:31956–63. [PubMed: 15145957]
6. Xu Y, Gurusiddappa S, Rich RL, Owens RT, Keene DR, Mayne R, et al. Multiple binding sites in collagen type I for the integrins alpha1beta1 and alpha2beta1. J Biol Chem. 2000; 275:38981–9. [PubMed: 10986291]
7. Salasznyk RM, Williams WA, Boskey A, Batorsky A, Plopper GE. Adhesion to Vitronectin and Collagen I Promotes Osteogenic Differentiation of Human Mesenchymal Stem Cells. J Biomed Biotechnol. 2004; 2004:24–34. [PubMed: 15123885]
8. Kundu AK, Putnam AJ. Vitronectin and collagen I differentially regulate osteogenesis in mesenchymal stem cells. Biochem Biophys Res Commun. 2006; 347:347–57. [PubMed: 16815299]
9. Ong SY, Wu J, Moochhala SM, Tan MH, Lu J. Development of a chitosan-based wound dressing with improved hemostatic and antimicrobial properties. Biomaterials. 2008; 29:4323–32. [PubMed: 18708251]
10. Arpornmaeklong P, Pripatnanont P, Suwatwirote N. Properties of chitosan-collagen sponges and osteogenic differentiation of rat-bone-marrow stromal cells. Int J Oral Maxillofac Surg. 2008; 37:357–66. [PubMed: 18272341]
11. Zhu Y, Liu T, Song K, Jiang B, Ma X, Cui Z. Collagen-chitosan polymer as a scaffold for the proliferation of human adipose tissue-derived stem cells. J Mater Sci Mater Med. 2009; 20:799–808. [PubMed: 19020954]
12. Çetinus ŞA, Şahin E, Saraydin D. Preparation of Cu(II) adsorbed chitosan beads for catalase immobilization. Food Chem. 2009; 114:962–9.
13. Nimni ME, Cheung D, Strates B, Kodama M, Sheikh K. Chemically modified collagen: a natural biomaterial for tissue replacement. J Biomed Mater Res. 1987; 21:741–71. [PubMed: 3036880]
14. Wang L, Stegemann JP. Thermogelling chitosan and collagen composite hydrogels initiated with beta-glycerophosphate for bone tissue engineering. Biomaterials. 2010; 31:3976–85. [PubMed: 20170955]
15. Song K, Qiao M, Liu T, Jiang B, Macedo HM, Ma X, et al. Preparation, fabrication and biocompatibility of novel injectable temperature-sensitive chitosan/glycerophosphate/collagen hydrogels. J Mater Sci Mater Med. 2010; 21:2835–42. [PubMed: 20640914]
16. Lavertu M, Filion D, Buschmann MD. Heat-induced transfer of protons from chitosan to glycerol phosphate produces chitosan precipitation and gelation. Biomacromolecules. 2008; 9:640–50. [PubMed: 18186608]
17. Hoemann CD, Chenite A, Sun J, Hurtig M, Serreqi A, Lu Z, et al. Cytocompatible gel formation of chitosan-glycerol phosphate solutions supplemented with hydroxyl ethyl cellulose is due to the presence of glyoxal. J Biomed Mater Res A. 2007; 83:521–9. [PubMed: 17503494]

18. Aalto-Korte K, Makela EA, Huttunen M, Suuronen K, Jolanki R. Occupational contact allergy to glyoxal. Contact Dermatitis. 2005; 52:276–81. [PubMed: 15899002]
19. Kiec-Swierczynska M, Krecisz B, Krysiak B, Kuchowicz E, Rydzynski K. Occupational allergy to aldehydes in health care workers. Clinical observations. Experiments. Int J Occup Med Environ Health. 1998; 11:349–58. [PubMed: 10028202]
20. Wang L, Singh M, Bonewald LF, Detamore MS. Signalling strategies for osteogenic differentiation of human umbilical cord mesenchymal stromal cells for 3D bone tissue engineering. J Tissue Eng Regen Med. 2009; 3:398–404. [PubMed: 19434662]
21. Wang L, Stegemann JP. Extraction of high quality RNA from polysaccharide matrices using cetlytrimethylammonium bromide. Biomaterials. 2009 Accepted.
22. Livak KJ, Schmittgen TD. Analysis of Relative Gene Expression Data Using Real-Time Quantitative PCR and the 2(-Delta Delta C(T)) Method. Methods. 2001; 25:402–8. [PubMed: 11846609]
23. Tippelt S, Ma C, Witt M, Bierbaum S, Funk RH. Collagen type I prevents glyoxal-induced apoptosis in osteoblastic cells cultured on titanium alloy. Cells Tissues Organs. 2004; 177:29–36. [PubMed: 15237193]
24. Redden RA, Doolin EJ. Collagen crosslinking and cell density have distinct effects on fibroblast-mediated contraction of collagen gels. Skin Res Technol. 2003; 9:290–3. [PubMed: 12877693]
25. Karamichos D, Skinner J, Brown R, Mudera V. Matrix stiffness and serum concentration effects matrix remodelling and ECM regulatory genes of human bone marrow stem cells. J Tissue Eng Regen Med. 2008; 2:97–105. [PubMed: 18338818]

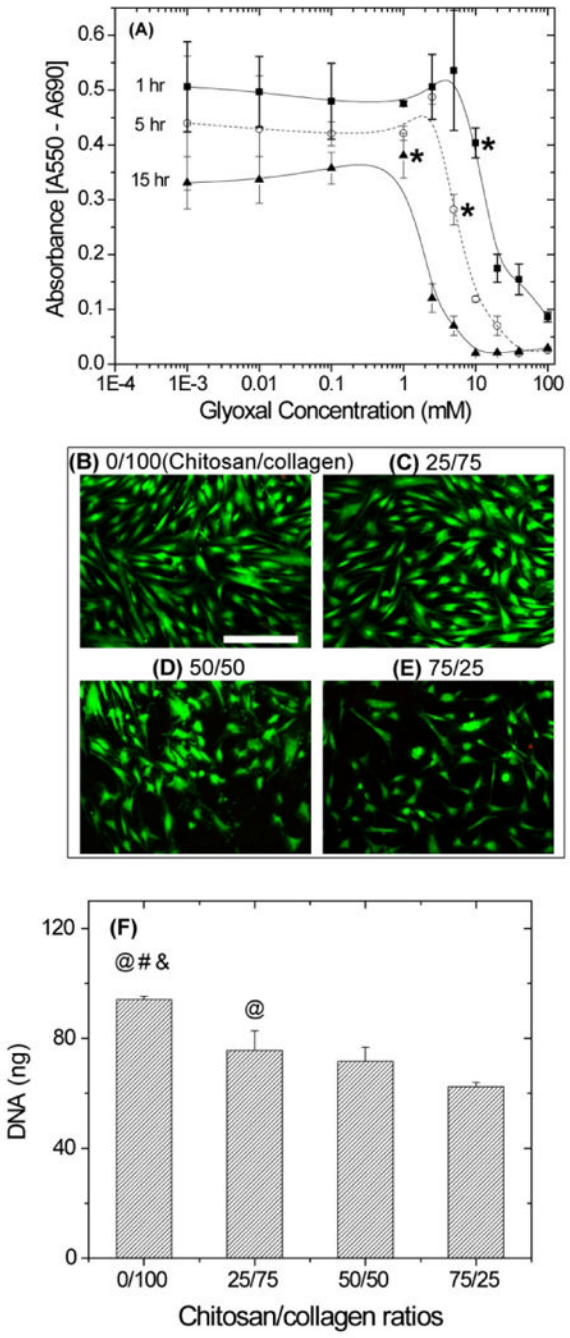


**Figure 1.**

Cytotoxicity studies of glyoxal showed that the effect on hBMSC metabolic activity (A) was both concentration- and time-dependent. Absorbance values in the control groups without glyoxal for 1, 5, and 15 hr were 0.45±0.03, 0.41±0.03 and 0.34±0.06, respectively. Vital staining (green indicates the cytoplasm live cells, red indicates the nucleus of dead cells) of hBMSC cultured on the surface of glyoxal crosslinked chitosan/collagen materials (B-E) showed that cell viability was not adversely affected by crosslinking of the matrix. The degree of hBMSC spreading (B-E) and increase in cell number as measured by DNA content (F) was dependent on substrate composition. Scale bar represents 200 μm. * = cut-off values after which hBMSC have significantly less metabolic activity than the control

groups ($p < 0.05$). @ = statistically significant difference from 75/25 group. # = statistically significant difference from 50/50 group. & = statistically significant difference from 25/75 group.

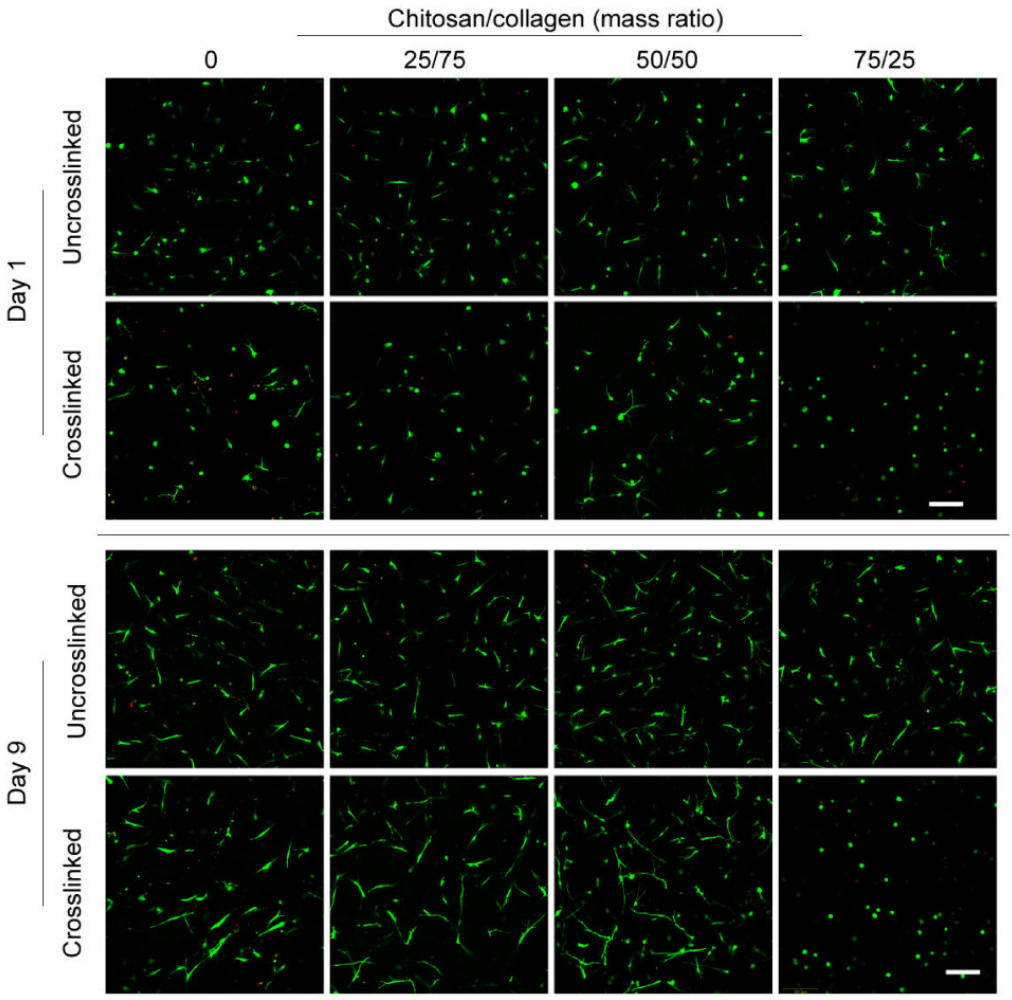


**Figure 2.**
Vital staining (green indicates the cytoplasm live cells, red indicates the nucleus of dead cells) of hBMSC embedded in 3D chitosan/collagen gels. Cells tolerated the glyoxal crosslinking process and maintained high cell viability during a 9-day culture period in all groups. Cell spreading inside the gels was evident in all groups by day 9, with the exception of the crosslinked 75/25 chitosan/collagen formulation. Scale bar represents 200 μm.

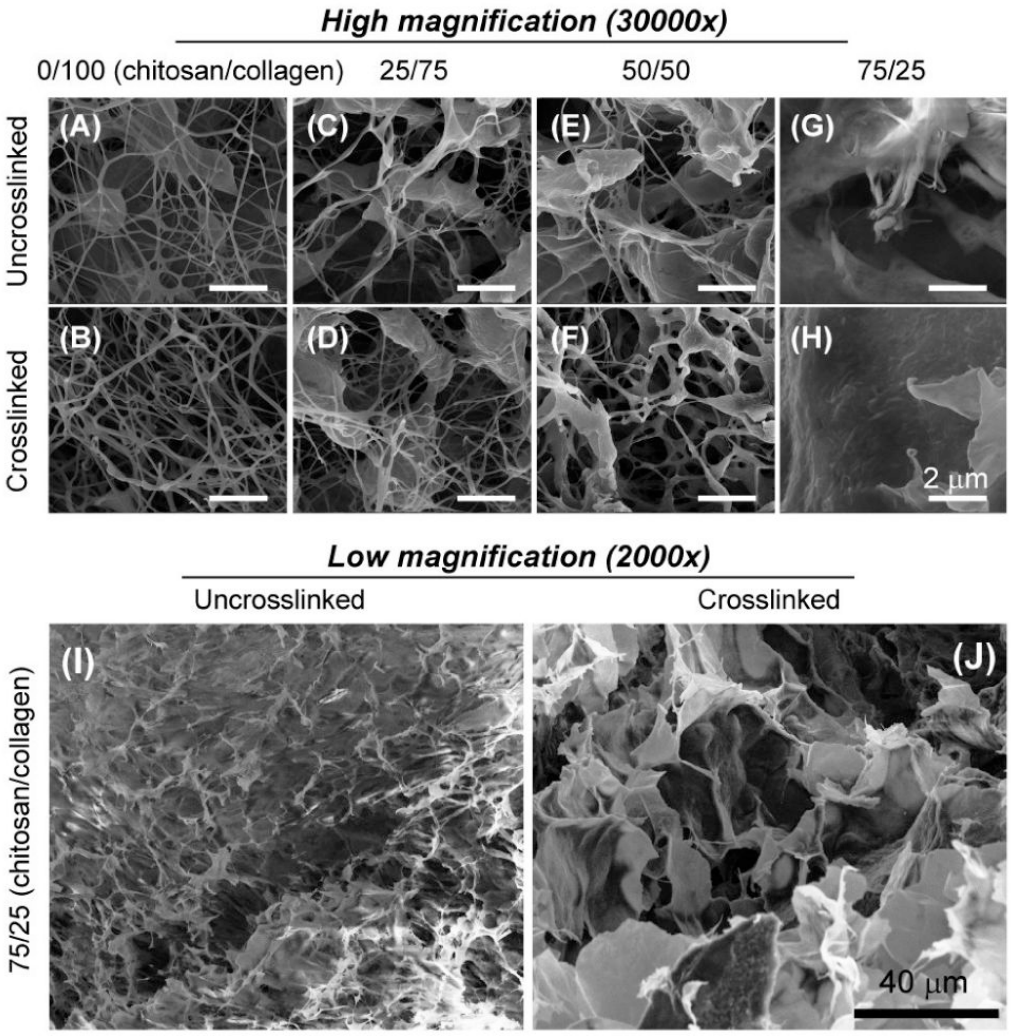


**Figure 3.**
Scanning electron microscopy images of chitosan/collagen composites revealed that matrix morphology changed from a fibrous network to a sponge-like morphology with increasing chitosan content.

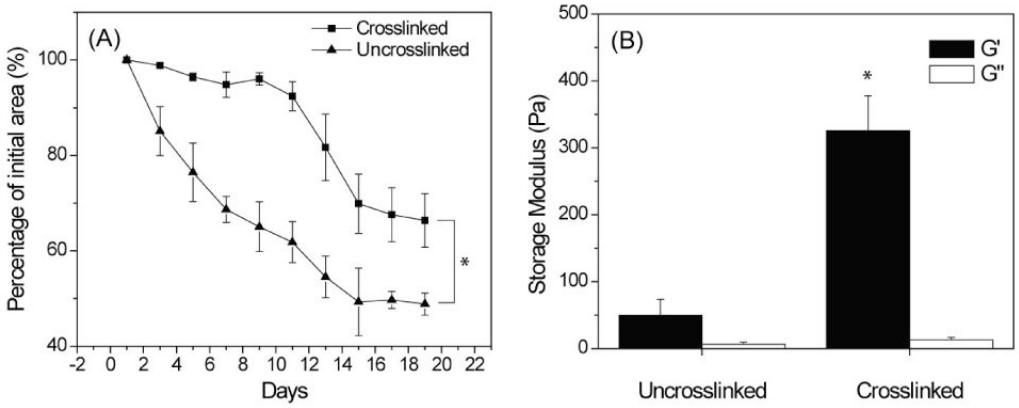


**Figure 4.**

Gel compaction (A) and rheological (B) tests of 50/50 chitosan/collagen composite materials showed a decreased gel compaction and increased matrix stiffness in the glyoxal crosslinked samples. * = statistically significant difference between crosslinked and uncrosslinked groups ($p<0.05$).

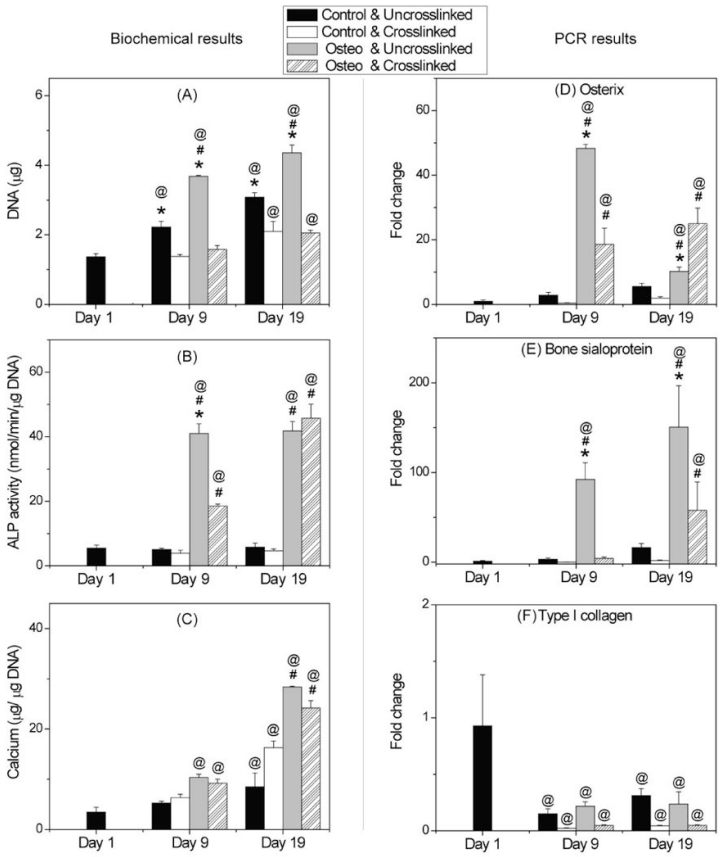


**Figure 5.**

DNA content (A), ALP activity (B), calcium content (C), and osteogenic gene expression (D-F) of hBMSC in uncrosslinked and crosslinked 50/50 chitosan/collagen gels. Cells proliferated more rapidly in uncrosslinked gels than in crosslinked gels, while both ALP activity and calcium content achieved a similar level by day 19. Osterix and bone sialoprotein genes were upregulated in osteogenic media, while type I collagen gene expression decreased during the culture period. * = statistically significant difference between uncrosslinked and crosslinked groups. # = statistically significant difference between control and osteogenic groups. @ = statistically significant difference from day 1.